HHS Public Access

Author manuscript

Proc SPIE Int Soc Opt Eng. Author manuscript; available in PMC 2013 December 16.

Published in final edited form as:

Proc SPIE Int Soc Opt Eng. 2013 March 6; 8668: 86685J–. doi:10.1117/12.2006280.

Image acquisition, geometric correction and display of images from a 2×2 x-ray detector array based on Electron Multiplying Charge Coupled Device (EMCCD) technology

S.N Swetadri Vasan[1,2,*], **P. Sharma**[1,2], **Ciprian N. Ionita**[2], **A.H. Titus**[1,2], **A.N. Cartwright**[1,2], **D.R Bednarek**[2], and **S. Rudin**[1,2]

[1]Department of Electrical Engineering, University at Buffalo

[2]Toshiba Stroke and Vascular Research Center, University at Buffalo

Abstract

A high resolution (up to 11.2 lp/mm) x-ray detector with larger field of view (8.5 cm × 8.5 cm) has been developed. The detector is a 2 × 2 array of individual imaging modules based on EMCCD technology. Each module outputs a frame of size 1088 × 1037 pixels, each 12 bits. The frames from the 4 modules are acquired into the processing computer using one of two techniques. The first uses 2 CameraLink communication channels with each carrying information from two modules, the second uses a application specific custom integrated circuits, the Multiple Module Multiplexer Integrated Circuit (MMMIC), 3 of which are used to multiplex the data from 4 modules into one CameraLink channel. Once the data is acquired using either of the above mentioned techniques, it is decoded in the graphics processing unit (GPU) to form one single frame of size 2176 × 2074 pixels each 16 bits. Each imaging module uses a fiber optic taper coupled to the EMCCD sensor. To correct for mechanical misalignment between the sensors and the fiber optic tapers and produce a single seamless image, the images in each module may be rotated and translated slightly in the x–y plane with respect to each other.

To evaluate the detector acquisition and correction techniques, an aneurysm model was placed over an anthropomorphic head phantom and a coil was guided into the aneurysm under fluoroscopic guidance using the detector array. Image sequences before and after correction are presented which show near-seamless boundary matching and are well suited for fluoroscopic imaging.

DESCRIPTION OF PURPOSE

Minimally invasive treatments of neurovascular pathology such as aneurysms, involve guiding a catheter to the region of treatment using x-ray fluoroscopic guidance. Once the catheter is deployed into the region near the aneurysm, treatment devices such as coils, balloons etc., are then deployed. These devices have small features which demand imaging detectors with very high spatial resolution. In order to address these concerns, a new high resolution x-ray detector based on EMCCD technology was developed (Fig 1)[1]. The

[*]The corresponding author is S.N. Swetadri Vasan, phone: 716-598-3915; ss438@buffalo.edu.

detector features an effective pixel size of 42.9 μm giving it a Nyquist frequency of 11.2 lp/mm which is significantly higher than the state of the art Flat Panel Detectors (FPD) detectors with Nyquist frequency of approximately 3.0 lp/mm. The field-of-view (FOV) for this new single-module detector is small, around 3 cm × 3 cm, and is dependent on the dimensions of the fiber optic taper used.

In order to achieve a bigger FOV but with the same high resolution, a 2 × 2 array of these modular detectors was developed [2]. The fiber optic tapers were fused (Fig 2) to achieve a field of view of about 8.5 cm × 8.5 cm with each detector having a Nyquist frequency of about 11.2 lp/mm. The sensors were mounted on individual headboards (Fig 3), and were aligned against the smaller end of the taper to form the array (Fig 4). The physical assembly of the camera is shown in Fig 5.

This paper presents the methods used to acquire the images from the 4 individual modules of the array and assemble them into one single frame. We also discuss how geometric corrections are preformed on the acquired images to present the user with one single complete frame. Although the field of view for the detector is about 8.5 cm × 8.5 cm, an x-ray FOV of 5 cm × 5 cm was demonstrated in this study since that was the size of the largest phosphor available to us at the time.

METHODS

Image Acquisition

The image from the array is acquired in two ways as described below in detail.

1) CameraLink—In base configuration mode, each CameraLink can support a transfer of 24 bits of data. Since the output of each camera module is 12 bits, 2 modules are connected to the 24 data bits of one camera link communication channel. Two such camera link channels are used to transfer the data from the camera to the computer. Fig 6 shows a data flow diagram of the communication channel.

In this configuration the frame grabber is programmed to collect the 24 bit data (2 chips × 1088 × 1037) from the CameraLink channel and convert it to a 32 bit image in memory. Each pixel in this 32 bit image consists of pixel information from 2 modules $E1_{11–0}$ and $E2_{11–0}$ (Fig. 7). Two 32 bit images from the two frame grabbers are sent to the Graphics Processing Unit (GPU), where the information from the individual pixels are extracted and rearranged to form one single 16 bit image of size 2176 × 2074 (2× 1088, 2× 1037).

2) Multiple Module Multiplexer Integrated Circuit (MMMIC)—Since the array consists of 4 detectors, 2 CameraLink channels can be used to transfer the information from the camera to the computer, but as the array size increases, increasing the number of CameraLink channels becomes impractical. So in order to address this communication issue a custom integrated circuit called MMMIC was developed and has been reported previously [3]. The basic functionality of this IC is to multiplex 3 channels into 1. A microphotograph of MMMIC is shown in Fig 8. For the 2×2 array a simple implementation of 3 MMMICs

were used to multiplex the data from four individual modules into one output channel (Fig 9).

Fig 10 shows a data flow diagram of the communication channel. In this configuration the frame grabber gets the data from the CameraLink channel and constructs it into a 16 bit image of size 4352 × 1037. In each row of the image, pixels 0,4,8… represent pixels 0,1,2 … from EMCCD #1 and pixels 1,5,9… represent pixels 0,1,2 … from EMCCD #2, pixels 2,6,10… represent pixels 0,1,2 … from EMCCD #3, and pixels 3,7,11… represent pixels 0,1,2 … from EMCCD #4. The image is sent to the GPU to be decoded and rearranged into one single 16 bit image of size 2176 × 2074 (2×1088, 2×1037).

For a 2×2 array, during one pixel readout time, four pixel values are multiplexed into one. So the MMMIC samples the input at a frequency four times faster than the pixel readout rate. But since the CameraLink is configured to grab an image of size 4352 × 1037 (i.e (4 × 1088) × 1037) the effective frame rate is the same as the pixel readout rate of one sensor.

Geometric Correction

The data acquired through either of the above mentioned methods is decoded in the GPU to form an image which depicts the image seen through the fiber optic tapers. The smaller end of the taper is smaller than the image area of the EMCCD chip. Thus the image from each module consists of the image transmitted through the taper as well as the parts of the active EMCCD image area that are not covered by the taper and are hence dark. Since the front end of the fiber optic taper is fused, the information going into the front end is received at the smaller ends of the tapers without any loss of information at the boundaries. There is a small mechanical misalignment between the EMCCD and the smaller end of the taper in each module, thus causing the image registered in the active area to be rotated and translated in x and y directions with respect to the other modules[4][5].

RESULTS

To evaluate the performance of the detector under clinical conditions an experiment was set up where an aneurysm model was placed over an anthropomorphic head phantom. A coil was guided into the aneurysm under fluoroscopy using the detector array. The detector entrance dose was measured to be around 15μR/frame with the technique parameters being 80 kVp tube potential, 32 mA tube current and 12.0 ms pulse width. Figures 11 a–c show the images from the sequence taken during the coiling procedure, after the acquired image is decoded in the GPU and before geometric correction. It can be seen that the image in each module is rotated and translated with respect to one another. The image of each individual module is corrected by rotating and translating in the x and y directions to obtain a near seamless image as shown in Figures 12 a–c

The salt and pepper noise seen in the outside part of each module's image in Figures 11 a–c is due to the use of a smaller than required phosphor which does not cover the full field of view. Thus when the flat field correction is made, this outside part of each module image becomes artifactual. Once we obtain a larger phosphor, these artifacts will not occur. Also for this reason only the central phosphor-covered parts of the processed images are shown in

Figures 12 a–c. The peripheral region was covered with a uniform grey for the convenience of the viewer.

CONCLUSIONS

From the image sequence shown in Figures 12 a–c, it can be concluded that with the different acquisition techniques and image corrections implemented, the 2×2 array of EMCCD based detectors can be used for real-time fluoroscopic interventions. The developed detector has a high resolution up to 11.2 lp/mm and a larger field of view, 8.5 cm × 8.5 cm. However, the design is extensible in both x and y directions, leading to even larger field of view detectors in the future.

References

1. Sharma P, Swetadri Vasan SN, Jain A, Panse A, Titus AH, Cartwright AN, Bednarek DR, Rudin S. EMCCD-based high resolution dynamic x-ray detector for neurovascular interventions. Conf Proc IEEE Eng Med Biol Soc. 2011; 2011:7787–90. [PubMed: 22256144]
2. Sharma P, Swetadri Vasan SN, Cartwright AN, Titus AH, Bednarek DR, Rudin S. Two dimensional extensible array configuration for EMCCD-based solid state x-ray detectors (2012). Medical Imaging 2012: Physics of Medical Imaging. Proceedings of the SPIE. 2012; 8313:83135A–12.
3. Sharma P, Swetadri Vasan SN, Titus AH, Cartwright AN, Bednarek DR, Rudin S. Implementation of Digital Multiplexing for High Resolution X-ray Detector Arrays. 2012 accepted for IEEE Eng Med Biol Soc.
4. Qu B, Huang Y, Wang W, Cartwright AN, Titus AH, Bednarek DR, Rudin S. Image geometric corrections for a new EMCCD-based dual modular x-ray imager. Conf Proc IEEE Eng Med Biol Soc. 2011; 2011:2634–7. [PubMed: 22254882]
5. Keleshis C, Hoffmann K, Lee J, Hamwi H, Wang W, Ionita C, Bednarek D, Verevkin A, Rudin S. Real-time implementation of distortion corrections for a tiled EMCCD-based Solid State X-ray Image Intensifier (SSXII). Proc Soc Photo Opt Instrum Eng. 2009; 7258:72583B1–72583B11.

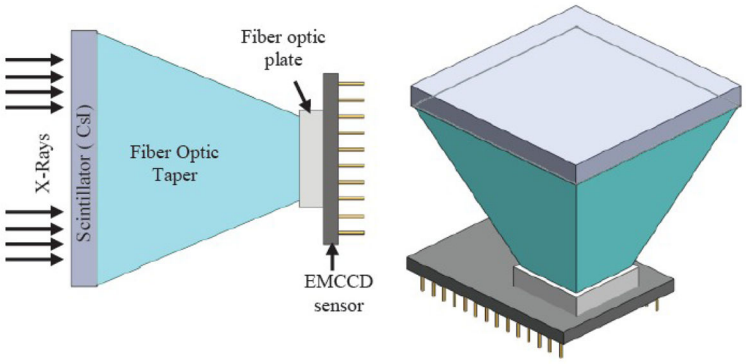

Figure 1.
Schematic diagram of a single module SSXII detector

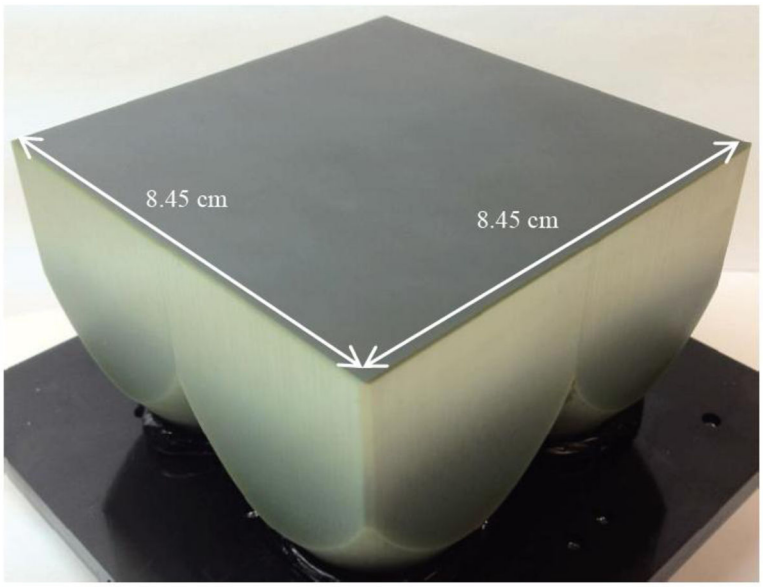

Figure 2.
Four detectors in a 2×2 arrangement

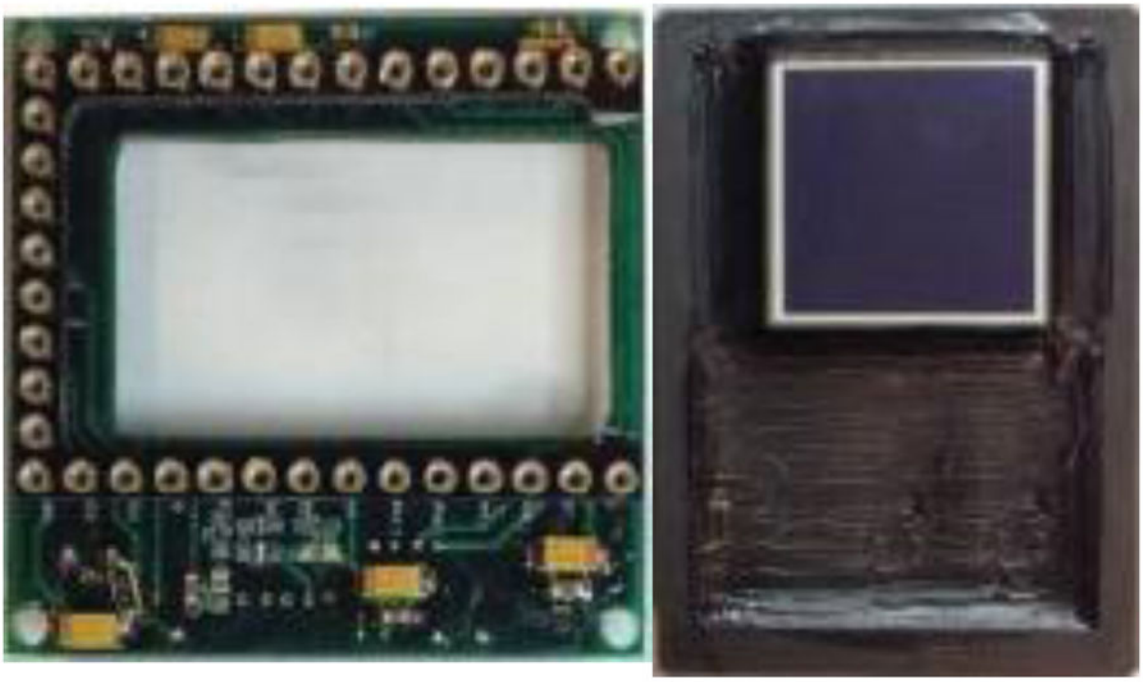

Figure 3.
Headboard for the sensor shown on theright.

Figure 4.
Rear view of a 2×2 assembly of the headboards, with sensors mounted on the front.

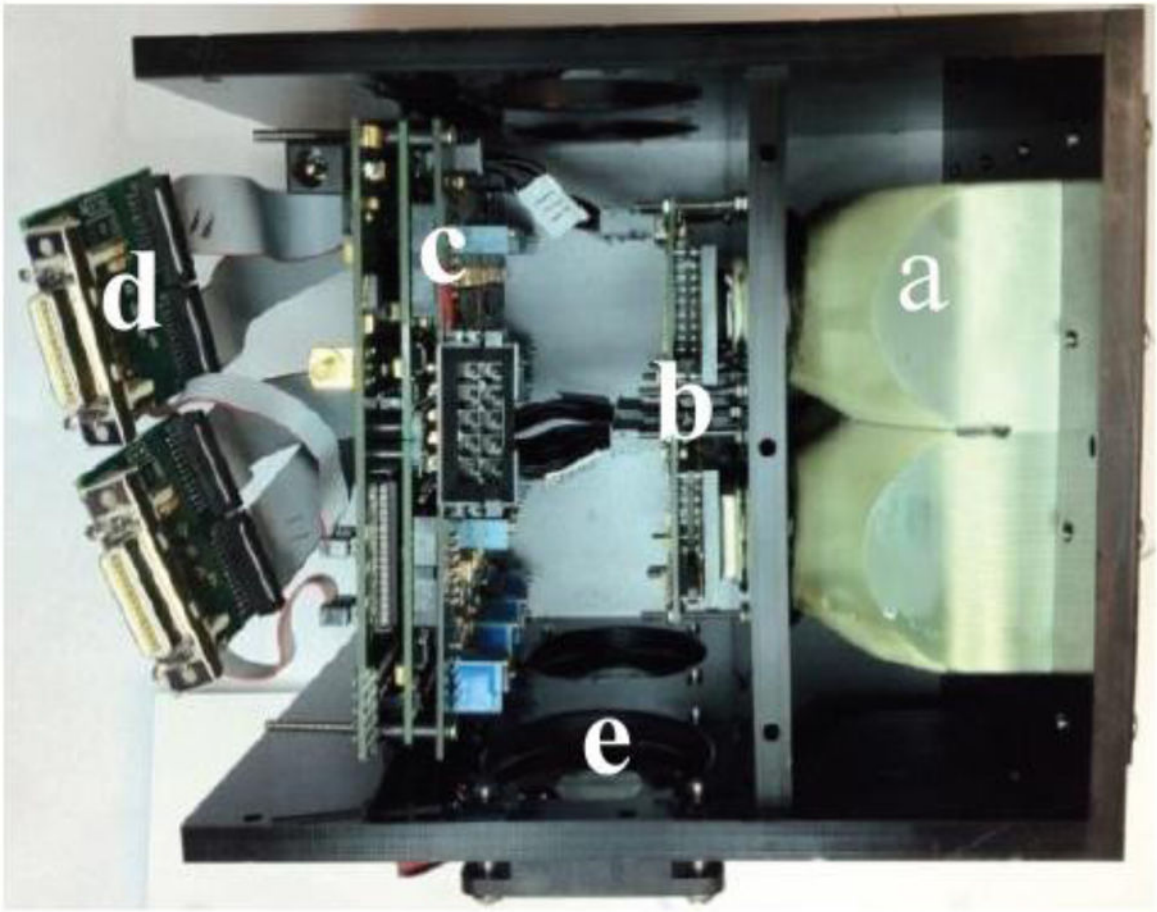

Figure 5.
Side view of complete assembly of 2×2 array. a) 2×2 fused taper assembly. b) 2×2 array of sensors mounted on individual headboards. c) Circuit boards to drive the sensors. d) CameraLink output e)Cooling assembly

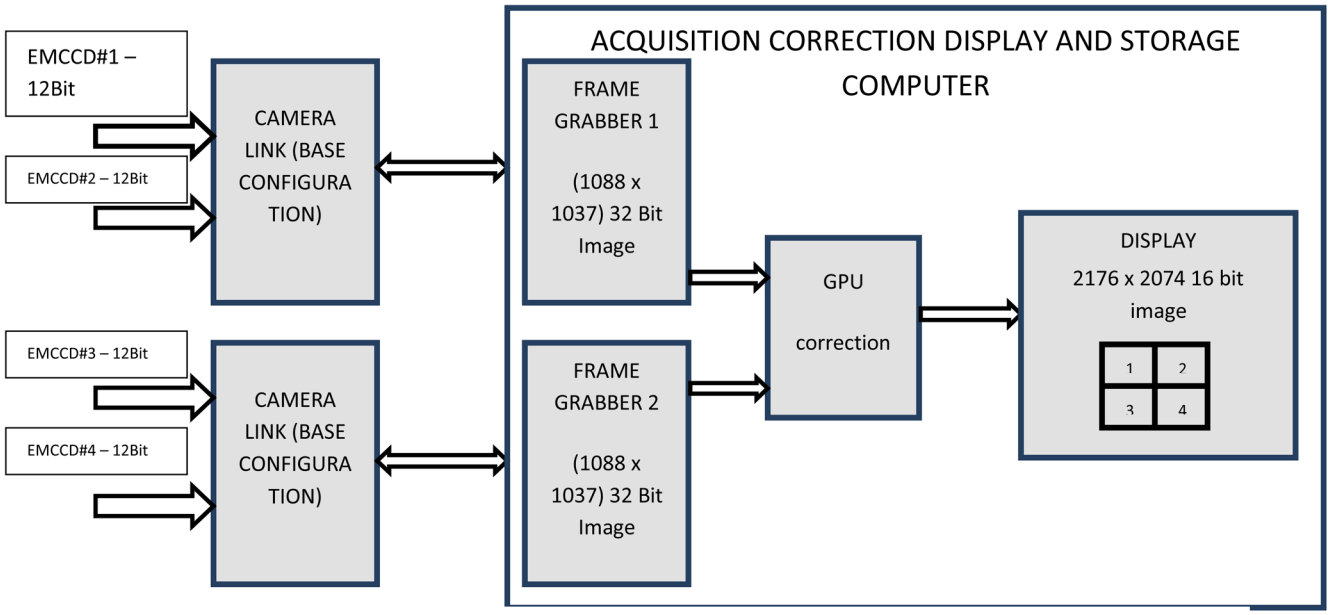

Figure 6.
Acquisition through 2 camera link channels; 4 modules are indicated

ALPHA CHANNEL	RED CHANNEL	GREEN CHANNEL	BLUE CHANNEL
0000 0000	$E1_7E1_6E1_5E1_4E1_3E1_2E1_1E1_0$	$E2_3E2_2E2_1E2_0E1_{11}E1_{10}E1_9E1_8$	$E2_{11}E2_{10}E2_9E2_8E2_7E2_6E2_5E2_4$

Figure 7.
One 32 bit pixel containing the bits from 2 modules

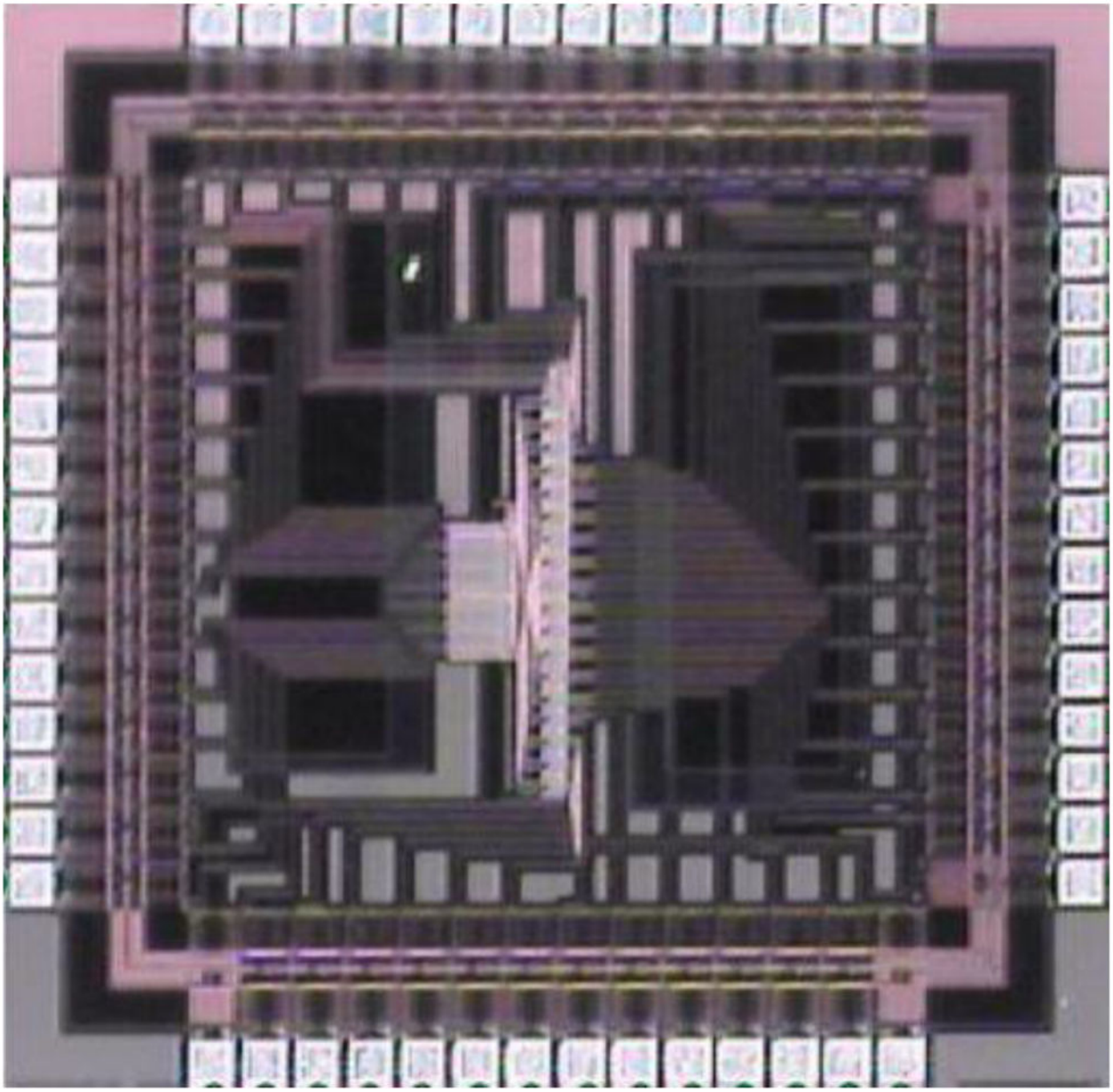

Figure 8.
A Microphotograph of MMMIC

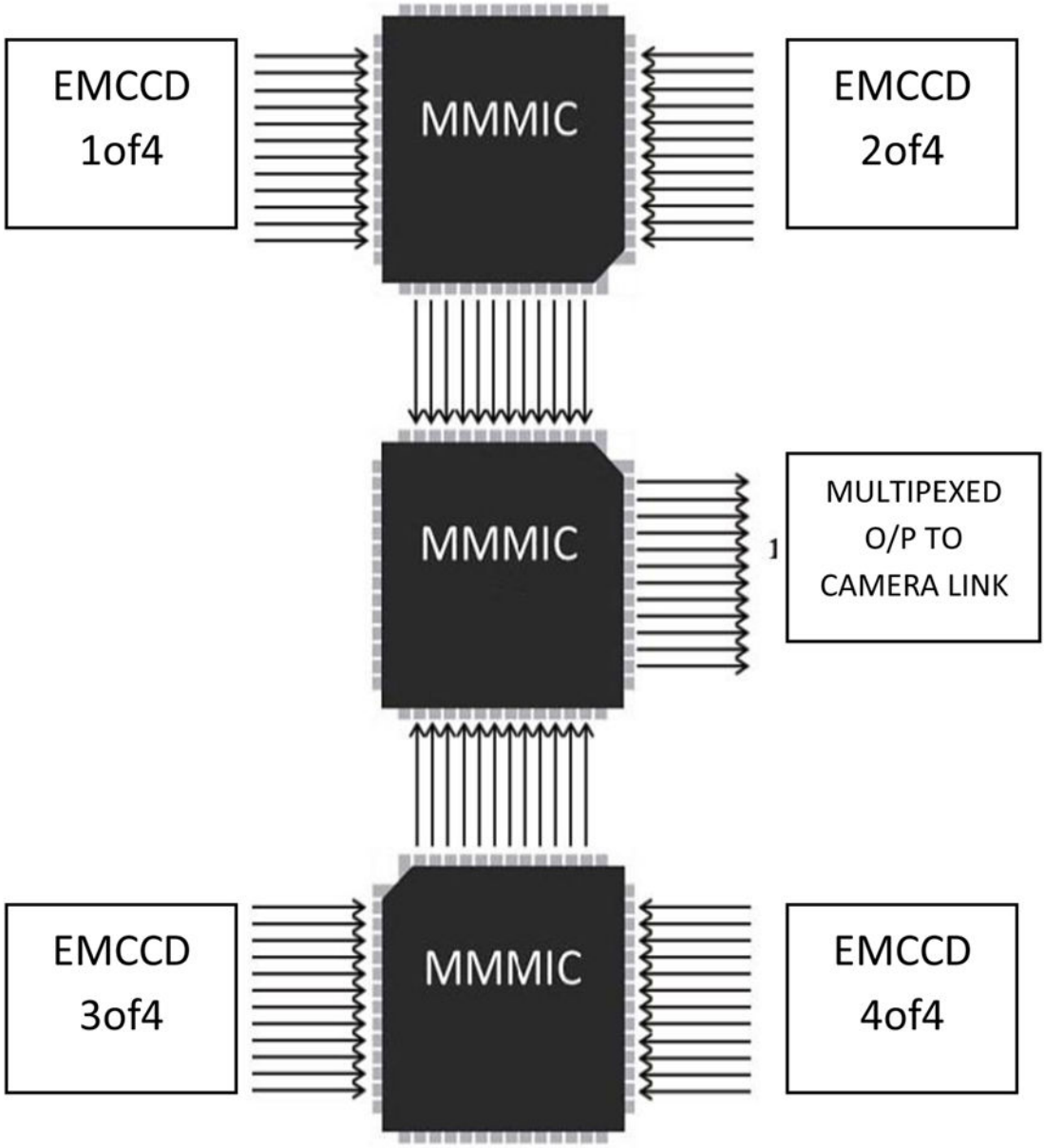

Figure 9.
MMMIC assembly to multiplex 4 channels into 1

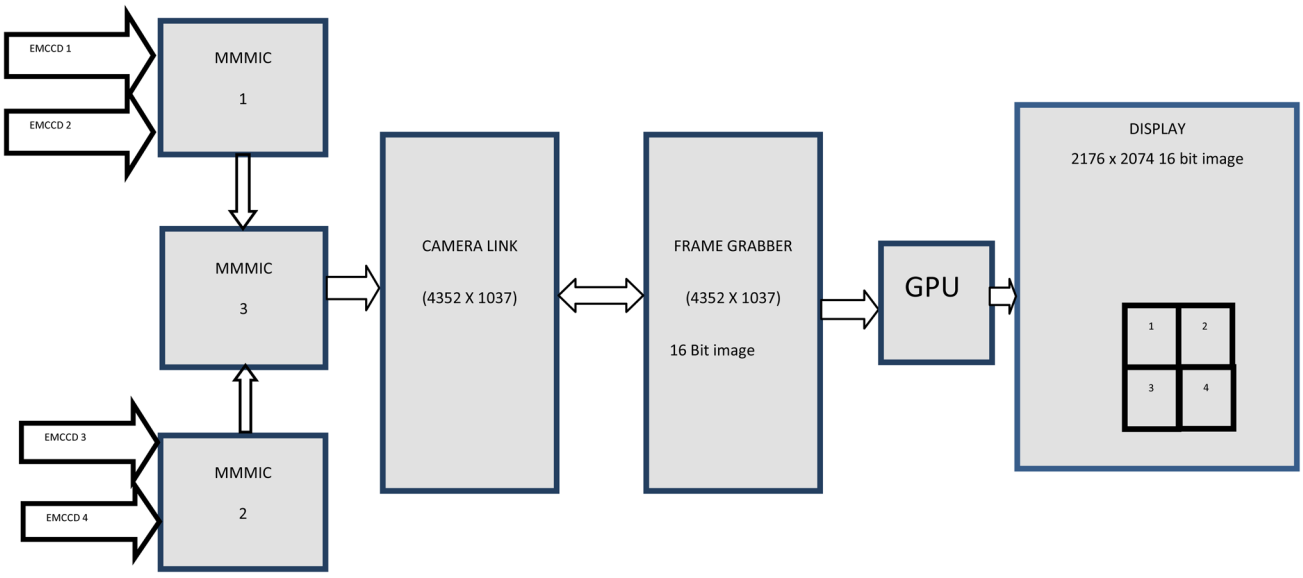

Figure 10.
Acquisition through MMMICs

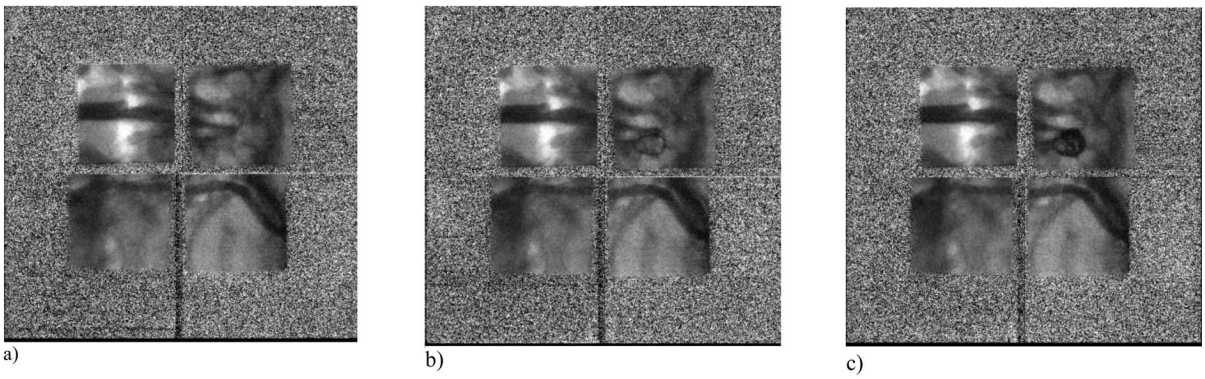

Figure 11.

Frames from image sequence before geometric correction:

a) beginning of coiling procedure.

b) Part of the coil inside the aneurysm

c) Coil filling the aneurysm

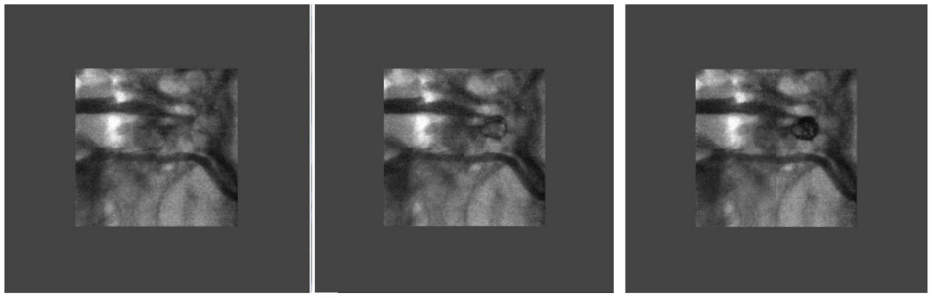

Figure 12.

Frames from image sequence after geometric correction:

a) beginning of coiling procedure,

b) Part of the coil inside the aneurysm,

c) Coil filling the aneurysm.